Supporting Information for

Modulation of Built-in Electric Field via Br Induced Partial Phase Transition for Robust Alkaline Freshwater and Seawater Electrolysis

Lei Jin, Hui Xu*, Kun Wang, Yang Liu, Xingyue Qian, Haiqun Chen*, Guangyu He*

Key Laboratory of Advanced Catalytic Materials and Technology, Advanced Catalysis and Green Manufacturing Collaborative Innovation Center, Changzhou University, Changzhou, Jiangsu Province 213164, China

Corresponding authors: xuhui006@cczu.edu.cn (H. Xu); hegy@cczu.edu.cn (G. He); chenhq@cczu.edu.cn (H. Chen)

1. Material characterizations

The crystal phases and structures of the as-prepared samples were characterized by powder X-ray diffraction (XRD) with Bruker D8 Advance diffractometer (Cu Ka radiation, $\lambda = 0.15418$ nm) in the 2θ range of 20-80° at a scanning rate of 0.05° s^{-1}. The microstructures of the products were observed by transmission electron microscopy (TEM, JEM-2100F) and field-emission scanning electron microscopy (FESEM, Zeiss Supra 55) that equipped with element mappings. The morphologies of the materials were characterized by scanning electron microscopy (SEM, Zeiss Sigma 300 Cold Field scanning electron microscope). X-ray photoelectron spectroscopy (XPS, PHI-5000C ESCA, PerkinElmer, USA) was employed to obtain elemental information of prepared catalysts on a VG ESCALAB MKII using Al Ka radiation. The Fourier transform infrared spectrometer (FT-IR, Nicolet iS5) was recorded to detect the functional groups of samples in the range of 200-2000 cm^{-1}. Ultraviolet photoelectron spectroscopy (UPS) is performed on Thermo ESCALAB Xi+ equipped with ultraviolet photoelectron spectrometer (Hel (21.22 eV)). Electron paramagnetic resonance (EPR) spectra were recorded on a Bruker EPR ELEXSYS 500 spectrometer. Inductively coupled plasma optical emission spectroscopy (ICP-OES) characterization was performed on an Agilent Varian 720ES equipment. Absorbance data of spectrophotometer were measured on UV-2700 spectrophotometer. Analysis of the molecular structure of the catalyst was performed using a Raman spectrometer (XPOLORA PLUS, China) at an excitation wavelength of 532 nm for Raman scattering peak analysis.

2. Electrochemical measurements

All the electrochemical measurements were tested using a CHI760E electrochemical workstation with a standard three electrode cell. The reference and counter electrodes were Hg/HgO and graphite rod, respectively. A glassy carbon electrode (GCE. 5 mm inner diameter) that modified with catalyst ink is used as the working electrode. The homogeneous catalyst ink was made by ultrasonically dispersing a mixture containing 2 mg of catalyst, 20 µL Nafion (5 wt%), 360 µL ethanol and 120 µL ultrapure water. Then, 13 µL of the catalyst ink was dropped on the surface of GCE. All potentials were measured against Hg/HgO and converted to reversible hydrogen electrode (RHE) by Nernst equation: $E_{vs\ RHE} = E_{vs\ Hg/HgO} + 0.0591 \cdot pH + 0.098$. The overpotential ($\eta$) was calculated through the formula: $\eta = E_{RHE} - 1.23$ V. Cyclic Voltammograms (CV) were measured at a scan rate of 5 mV/s. Electrochemical impedance spectroscopy was tested over the frequency range of 1000000 to 0.01 Hz with an AC signal amplitude of 5 mV. The double-layer capacitance (C_{dl}) was evaluated by cyclic voltammetry (CV) curves performed at the non-faraday reaction regions with an interval of 20 mV/s over the scanning range of 20 ~ 120 mV/s. The turnover frequency (TOF) values were calculated from the following equation: $TOF = (j \times A)/ (k \times F \times n)$. Here, k is the number of electron transfer (the factors of HER and OER are respectively 2 and 4), j is the current density at a given overpotential, A is the geometric surface area of the electrode, F is the Faraday constant (96485.3 C/mol), n is the number of active sites (mol). The number of voltammetric charges is gained by CV curves from -0.6 ~ 0 V and 0 ~ 0.6 V *vs.*

RHE for OER and HER in phosphate buffer solution (pH = 7) with a scan rate of 50 mV/s respectively, and the following equation is n (mol) = Q/2F (the surface charge Q is proportional to the number of active sites). The long-term stability of the catalyst was conducted by chronopotentiometry (CP). All the data of electrochemistry were presented without any iR correction.
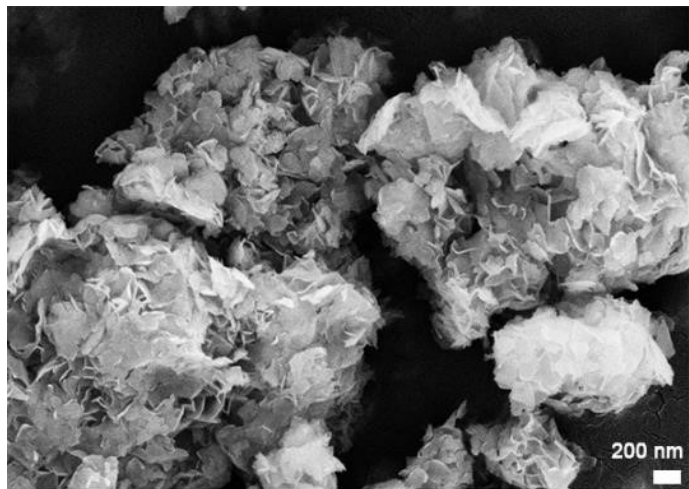
Fig. S1 SEM image of the NiFe LDH.
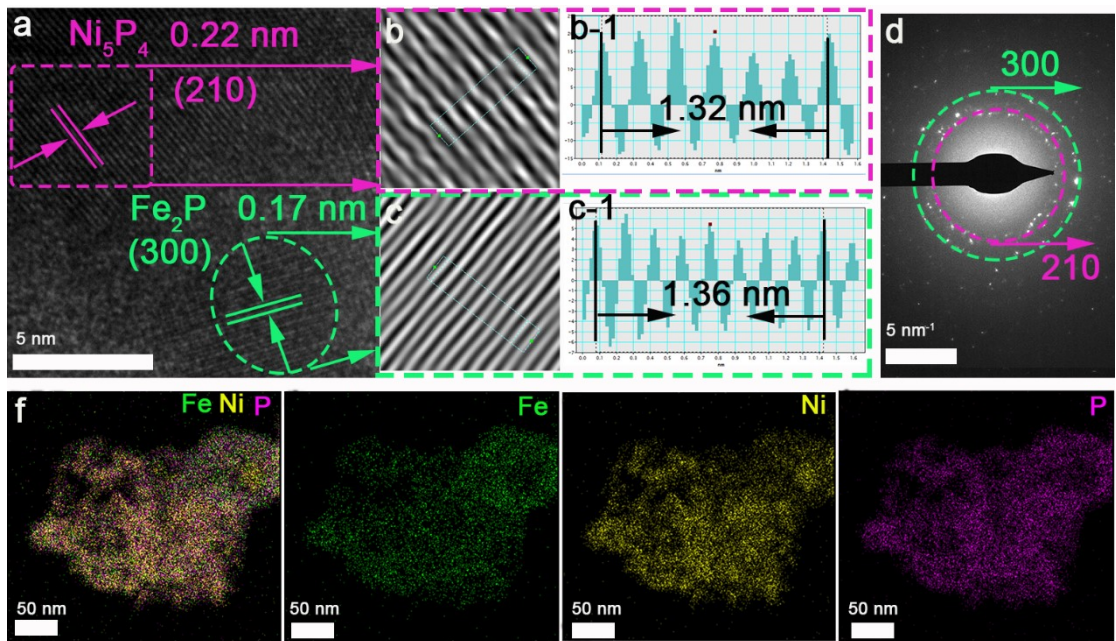
Fig. S2 (a-c) High-resolution TEM of Fe$_2$P/Ni$_5$P$_4$, integrated pixel intensities (b-1 and c-1) of Ni$_5$P$_4$ and Fe$_2$P (taken from the green dotted rectangle in (b) and (c)). (d) SAED pattern of Fe$_2$P/Ni$_5$P$_4$. (f) Mapping images of Fe$_2$P/Ni$_5$P$_4$
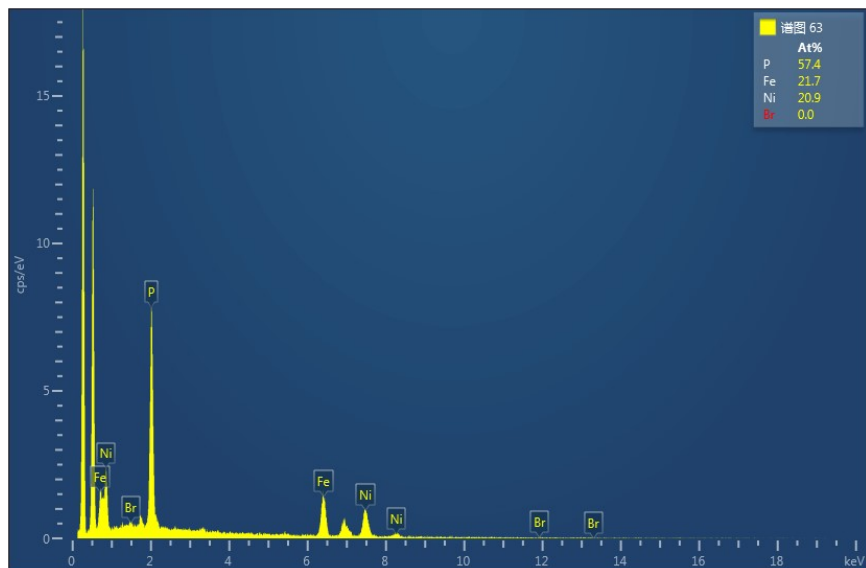
Fig. S3 EDX spectrum of Fe$_2$P/Ni$_2$P.
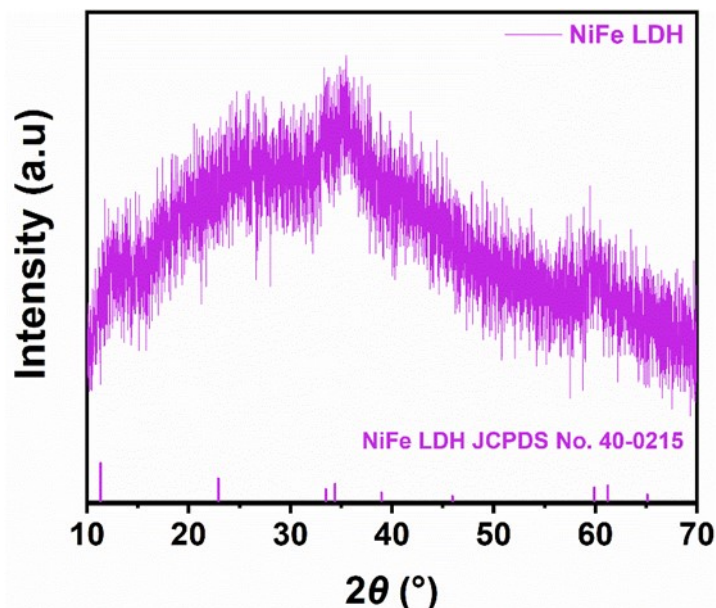
Fig. S4 XRD patterns of NiFe LDH

Table S1 UPS measured work functions of Fe_2P, Ni_5P_4 and Ni_2P

Catalysts	E_{cutoff} (eV)	E_{VB} (eV)	Φ (eV)
Fe_2P	15.0	2.47	6.22
Ni_5P_4	15.3	3.96	5.92
Ni_2P	14.5	3.67	6.72
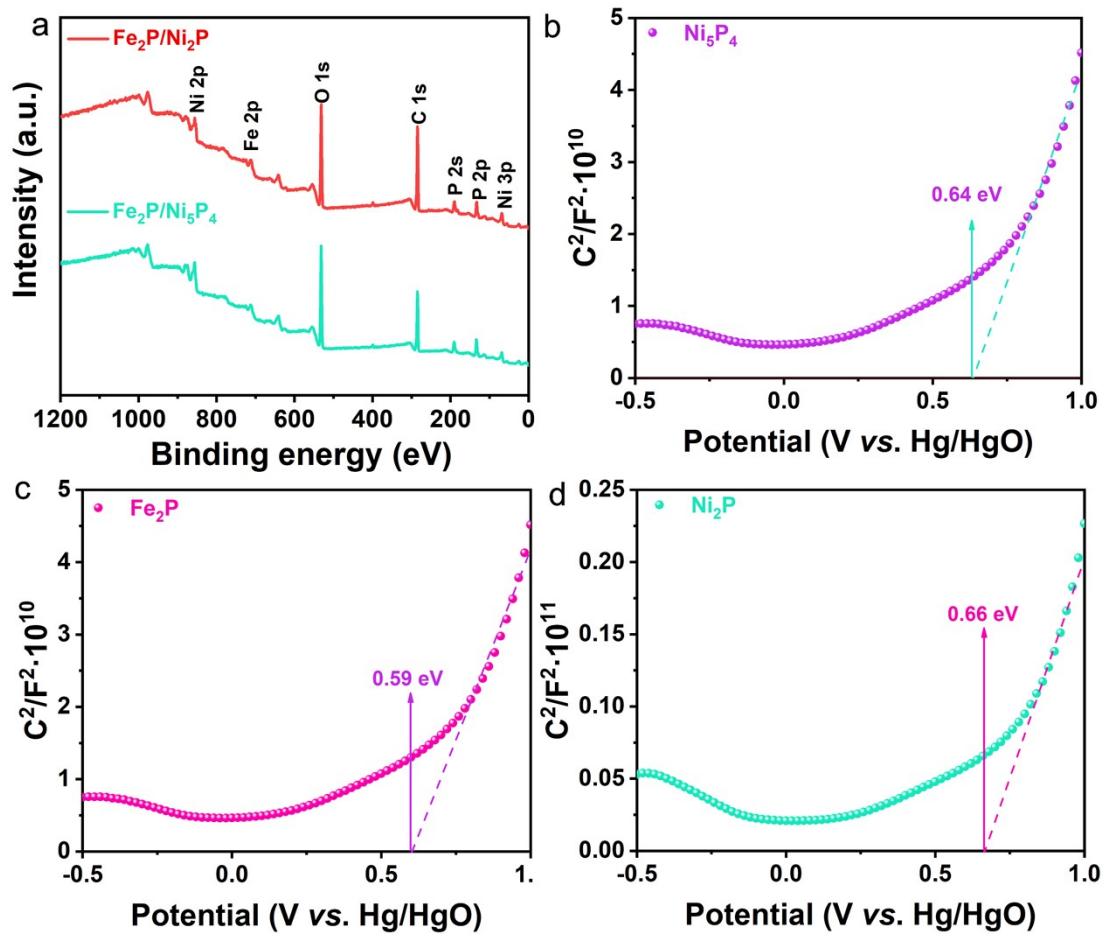
Fig. S5 (a) XPS survey spectra of the Fe_2P/Ni_2P and Fe_2P/Ni_5P_4. Mott-Schottky plots of (b) Ni_5P_4, (c) Fe_2P, and (d) Ni_2P.
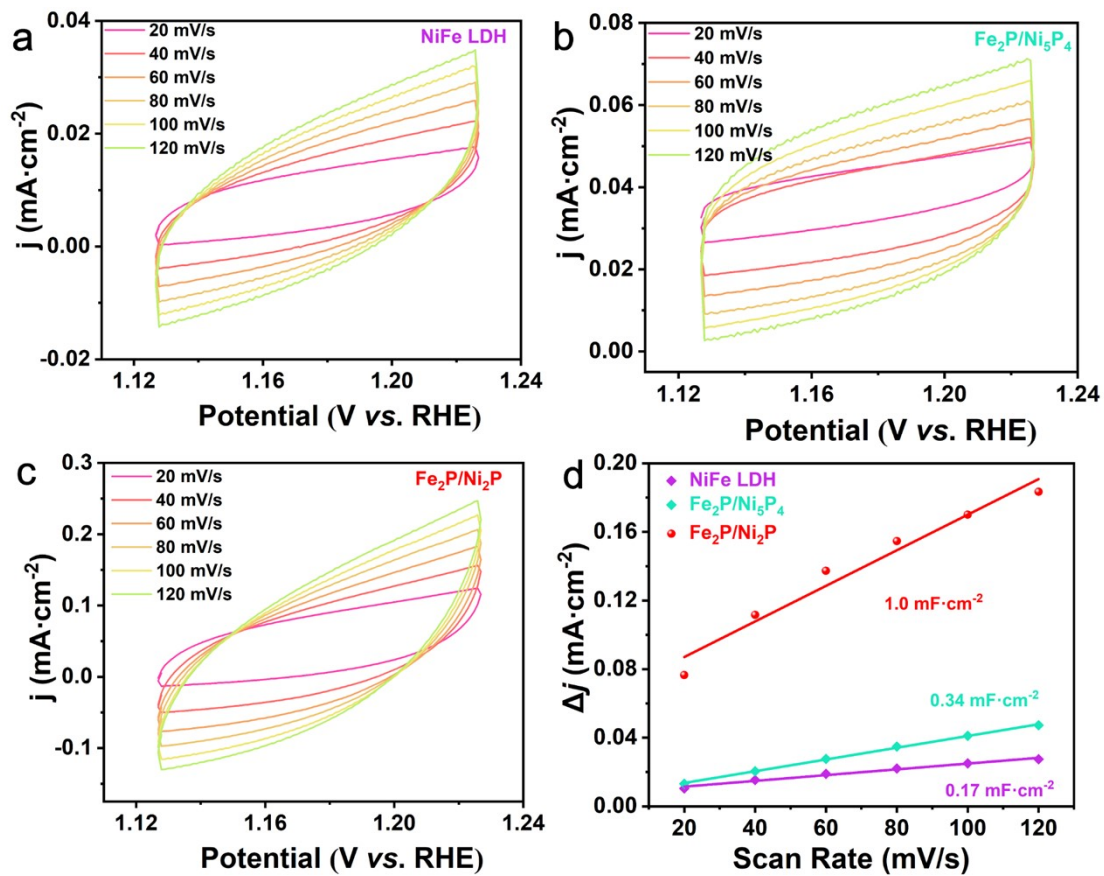
Fig. S6 (a-c) CV curves of different electrocatalysts with different scanning rates for OER in 1.0 M KOH solution. (d) C_{dl} values of different catalysts for OER in 1.0 M KOH solution.
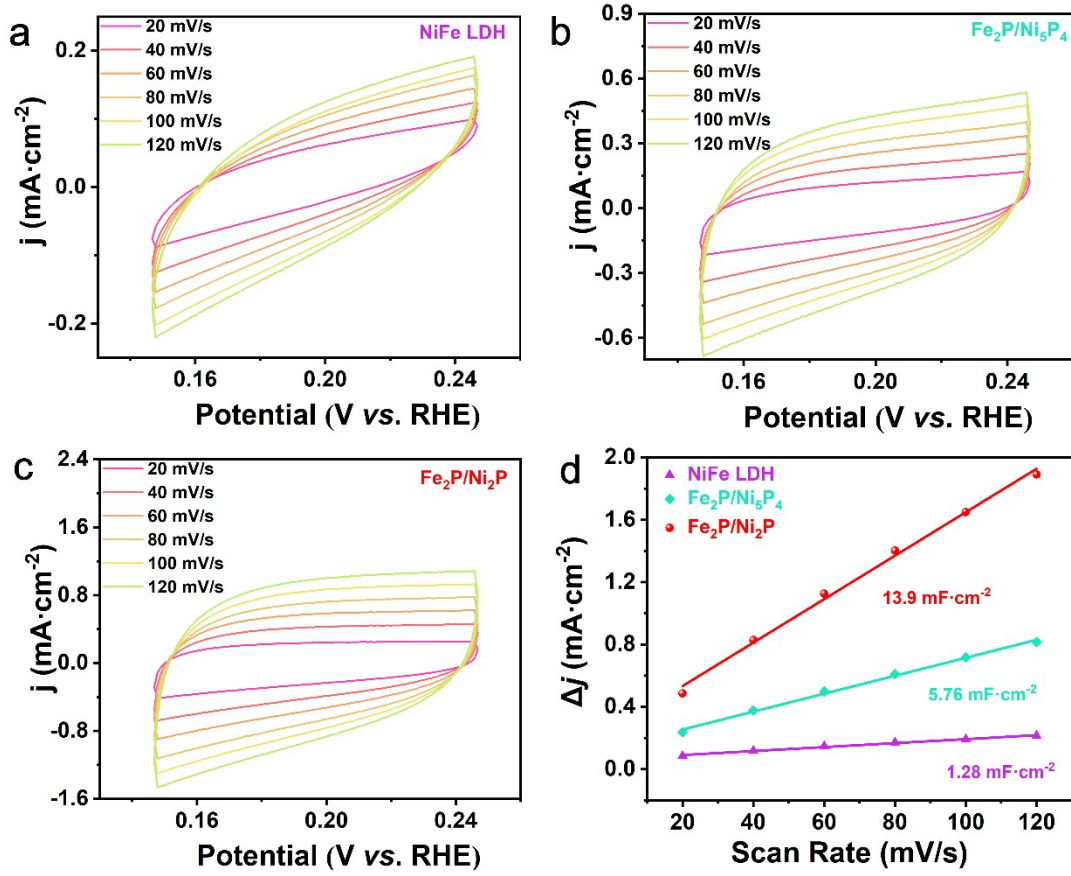
Fig. S7 (a-c) CV curves of different electrocatalysts with different scanning rates for HER in 1.0 M KOH solution. (d) C_{dl} values of different catalysts for HER in 1.0 M KOH solution.
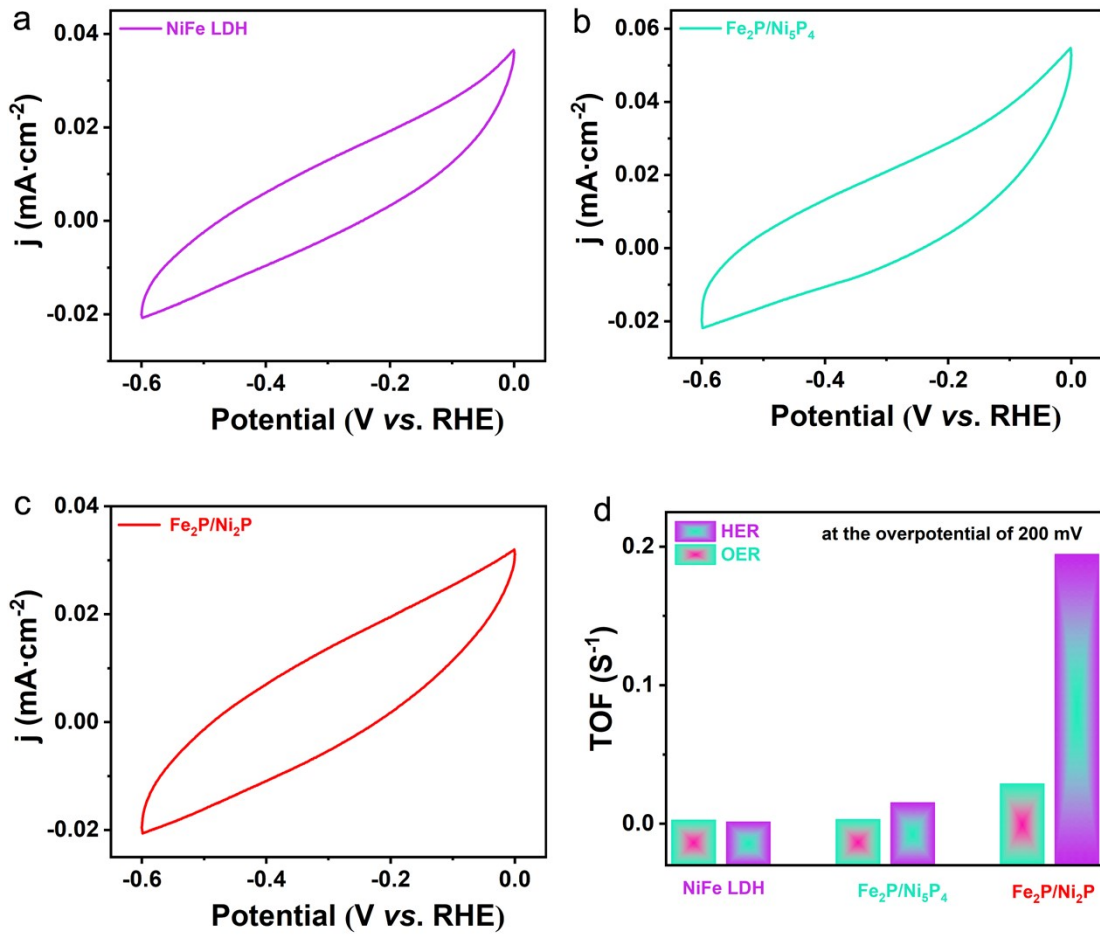
Fig. S8 (a-c) CV curves from -0.6 to 0 V *vs.* RHE for OER in 1.0 M PBS (pH = 7) at 50 mV s^{-1}. (d) TOF values of different catalysts for OER and HER in 1.0 M KOH + freshwater solution.
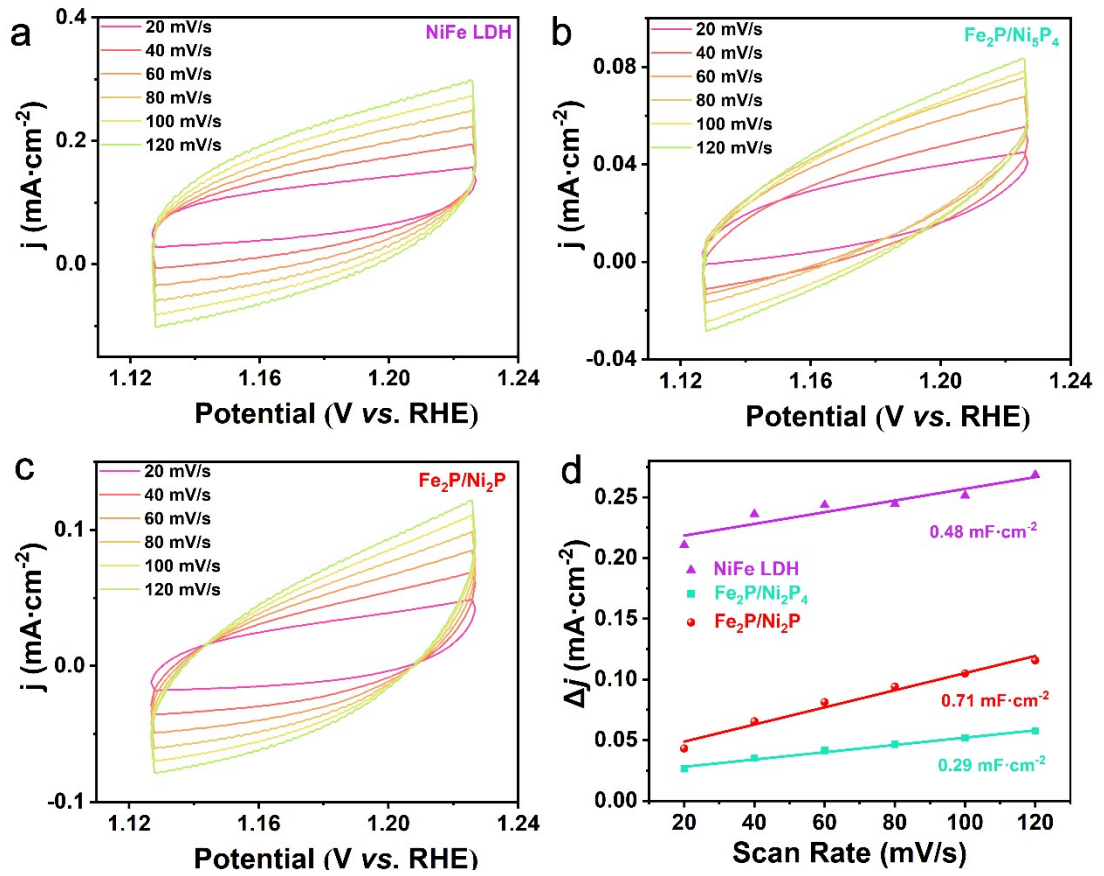
Fig. S9 (a-c) CV curves of different electrocatalysts with different scanning rates for OER in alkaline seawater solution. (d) C_{dl} values of different catalysts for OER in alkaline seawater solution.
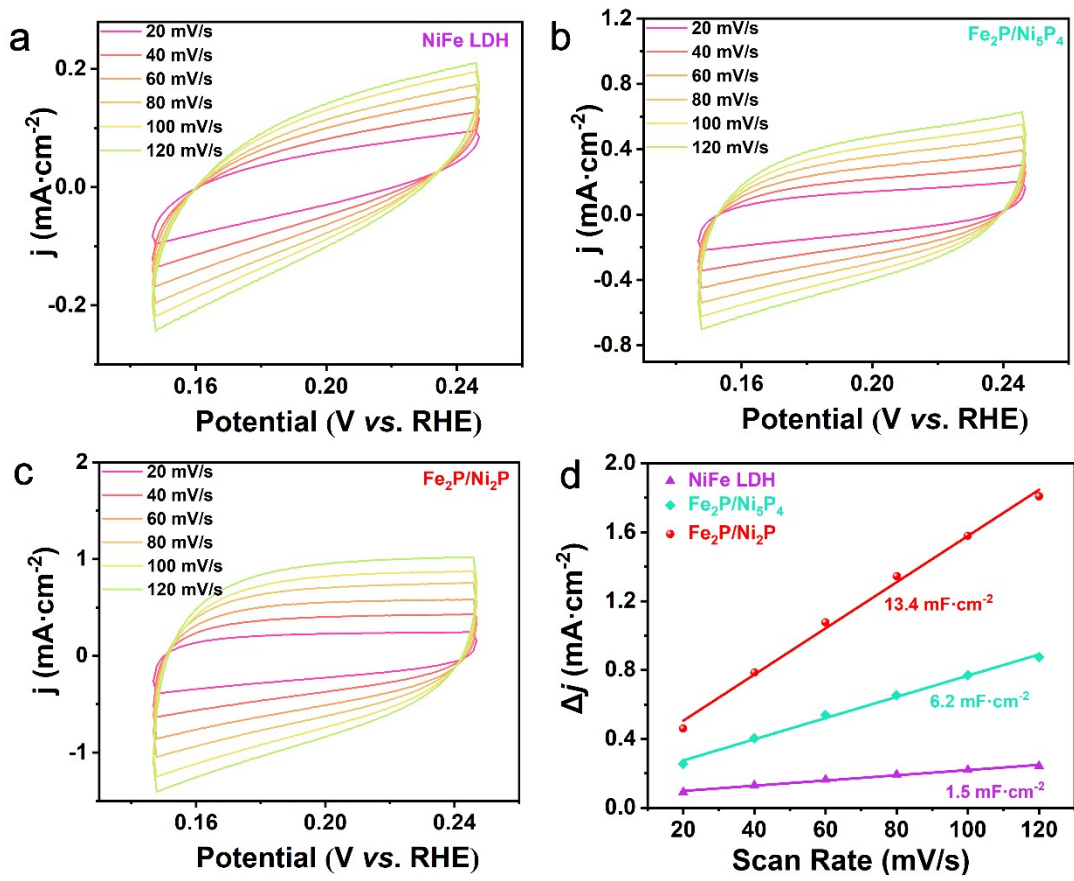
Fig. S10 (a-c) CV curves of different electrocatalysts with different scanning rates for HER in alkaline seawater solution. (d) C_{dl} values of different catalysts for HER in alkaline seawater solution.
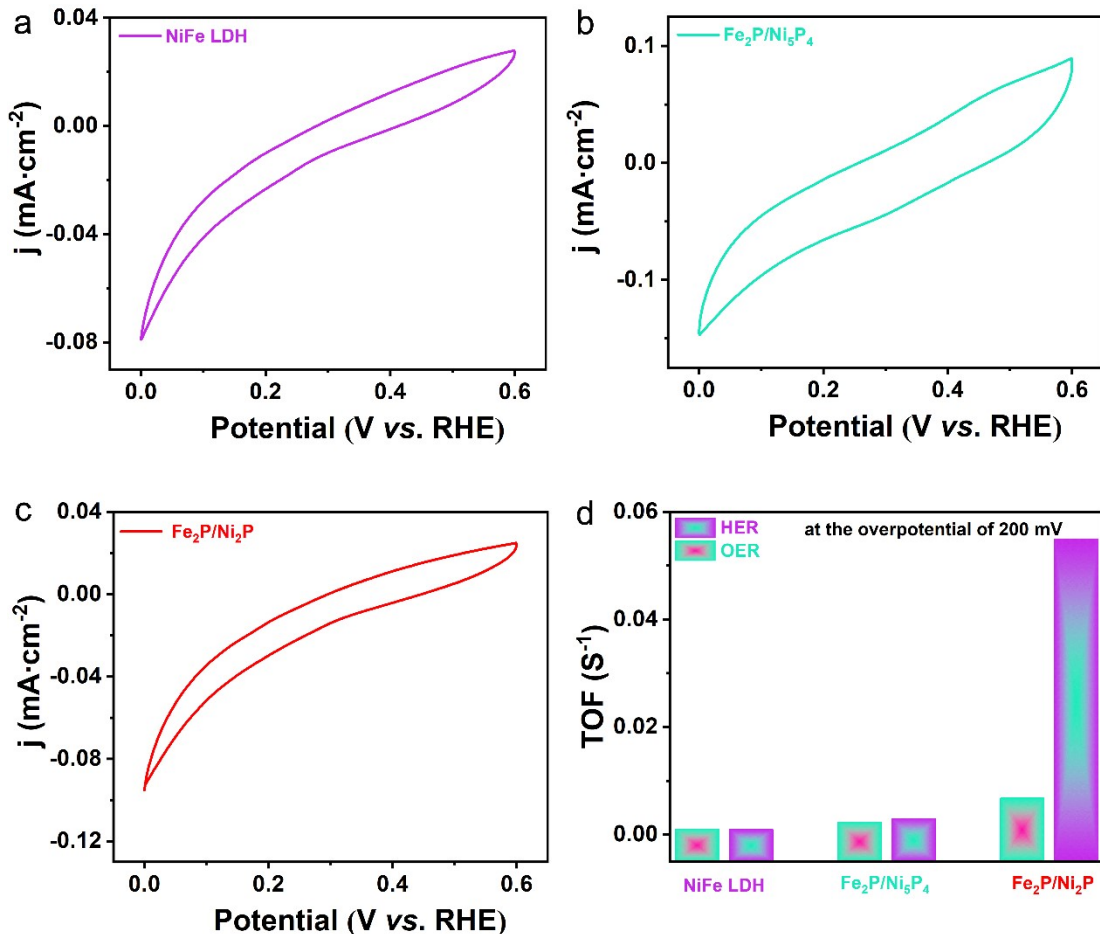
**Fig. S11** (a-c) CV curves from 0 ~ 0.6 V *vs.* RHE for OER in 1.0 M PBS (pH = 7) at 50 mV s^{-1}. (d) TOF values of different catalysts for OER and HER in 1.0 M KOH + seawater solution.
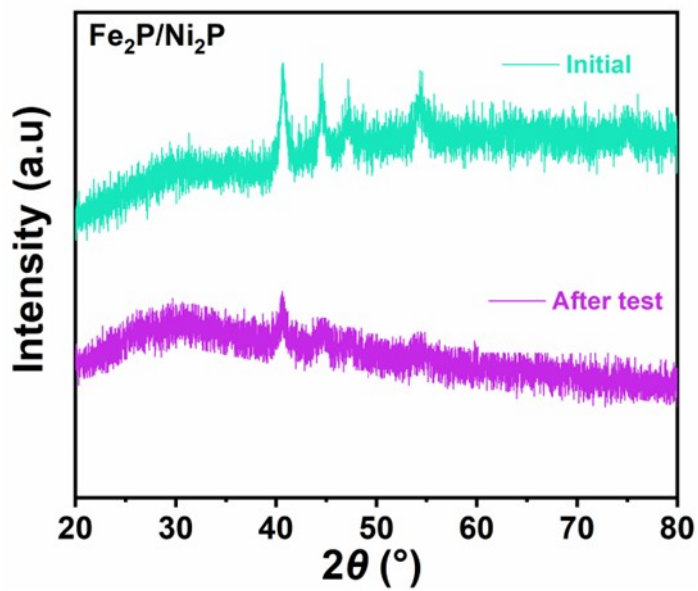
Fig. S12 XRD pattern of the Fe_2P/Ni_2P catalyst before and after the test.
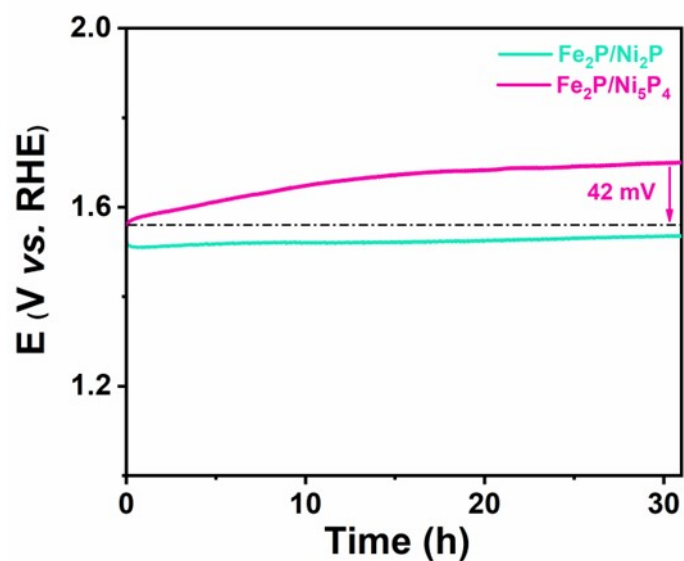
Fig. S13 Electrolytic alkaline seawater oxidation lifespan comparison of Fe_2P/Ni_2P and Fe_2P/Ni_5P_4 at 50 mA cm^{-2}.
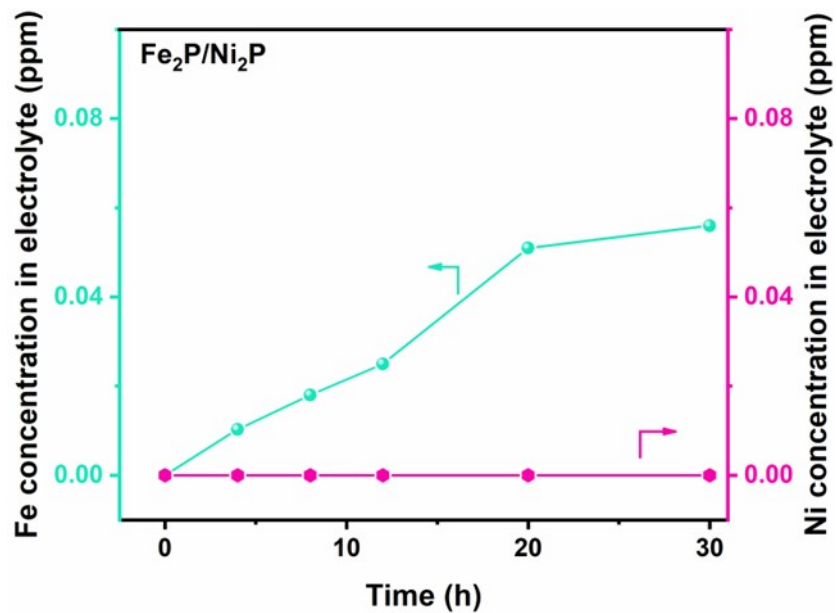
Fig. S14 Concentrations of Fe and Ni versus reaction time for Fe$_2$P/Ni$_2$P.
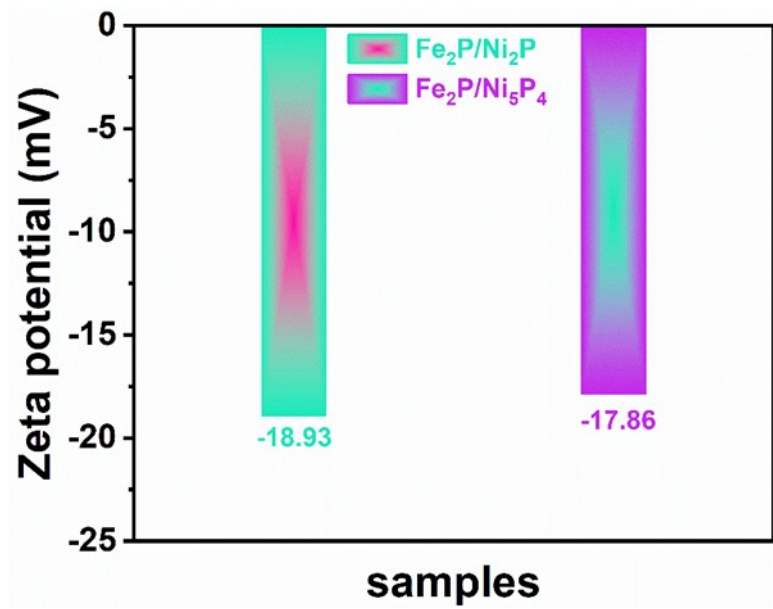
Fig. S15 Zeta potential values of Fe_2P/Ni_5P_4 and Fe_2P/Ni_2P.
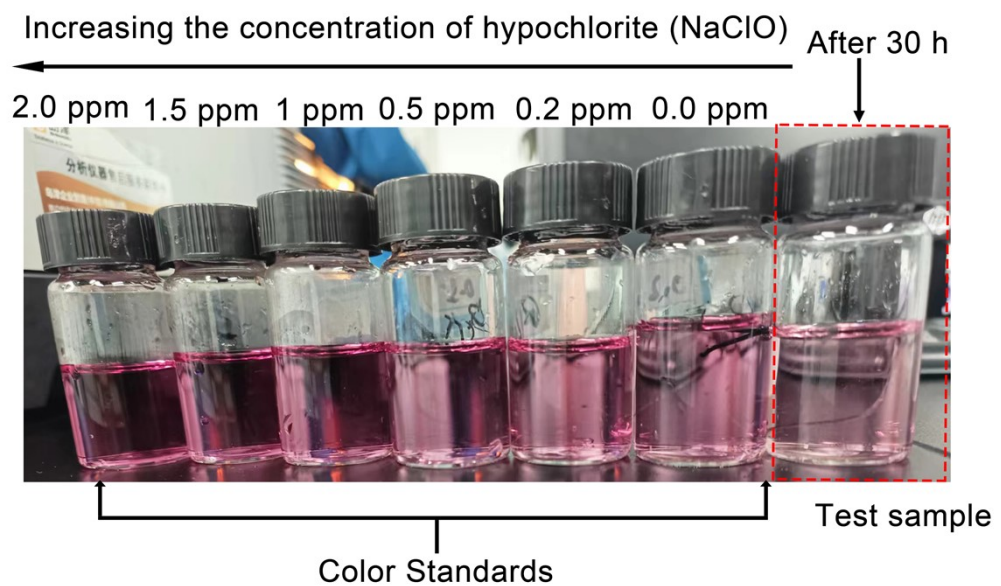
Fig. S16 Hypochlorite detection result with different NaClO contents and the electrolyte after 30 h electrolysis for Fe_2P/Ni_2P at a constant current density of 50 mA cm^{-2} in 1 M KOH + seawater.
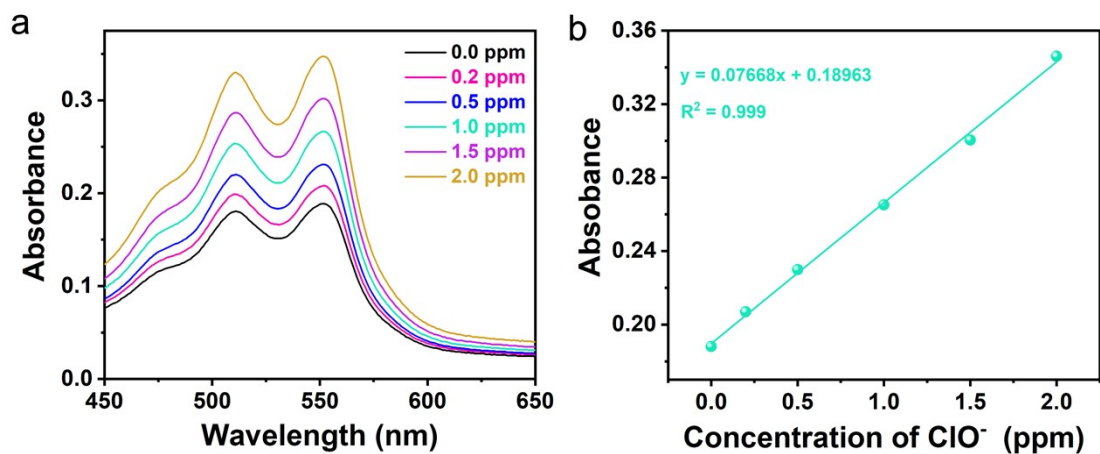
Fig. S17 (a) UV-Vis absorption spectra of ClO⁻ with different concentrations. (b) Calibration curve used for calculating ClO⁻ concentrations of the electrolyte.
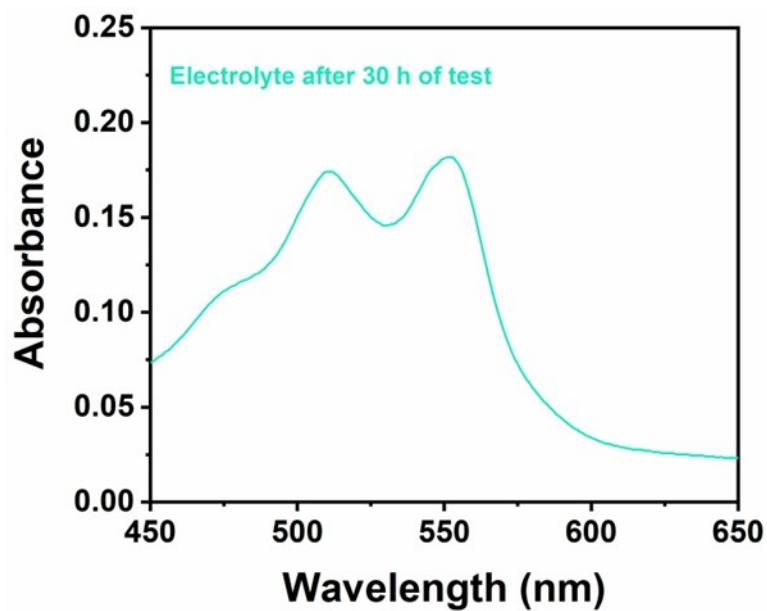
Fig. S18 UV/Vis absorption spectrum of the electrolyte after 100 h electrolysis for Fe$_2$P/Ni$_2$P at a constant current density of 50 mA cm^{-2} in 1 M KOH + seawater.
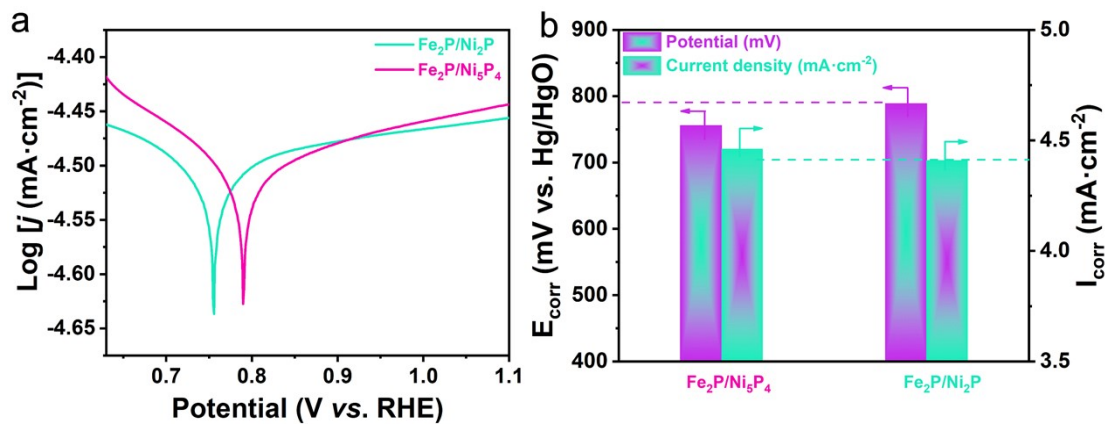
Fig. S19 (a) Polarization curves for corresponding electrodes after OCP test. (b) comparison of Ecorr and Icorr on Fe_2P/Ni_5P_4 and Fe_2P/Ni_2P.
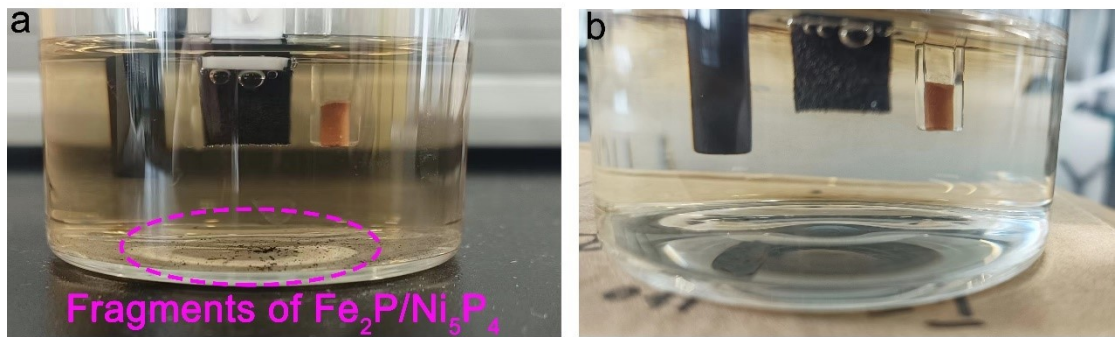
Fig. S20 Photographs of (a) Fe$_2$P/Ni$_5$P$_4$ and and (b) Fe$_2$P/Ni$_2$P during alkaline seawater electrolysis. The fragment of Fe$_2$P/Ni$_5$P$_4$ would severely drop as a result of instability.

Table S2 Comparison of OER performance in 1.0 M KOH solution for Fe_2P/Ni_2P with some representative catalysts.

Catalysts	Overpotential (mV)	Current density (mA cm^{-2})	Ref
Fe_2P/Ni_2P	196	**10**	**This work**
CoP_2/NC-1	290	10	1
Ir@Zr-CoP	292	10	2
Ru-MoCoP	240	10	3
Ni_2P/Ni_5P_4	286	10	4
CoP@CNF	300	10	5
CoP/NiCoP	310.7	10	6
CoP/Mo_2CT_x	312	10	7
$Ru-RuP_xCo_xP$	338	10	8
Fe-Co-P	340	10	9
Mn-CoP-2	344	10	10
V-CoP	420	10	11

Table S3 Comparison of HER performance in 1.0 M KOH solution for Fe_2P/Ni_2P with some representative catalysts reported.

Catalysts	Overpotential (mV)	Current density (mA cm^{-2})	Tafel slope (mV/dec)	Ref.
Fe_2P/Ni_2P	**108**	**10**	**121.5**	**This work**
Co-P-O$_2$	113	10	49	12
Co-Ni-P/MoS$_2$	116	10	41	13
V-dope-MoS$_2$	206	10	89	14
NiCoSe|S/BP	172	10	128	15
NiSe@Co$_{0.85}$Se/NF	168	10	72	16
Co$_{0.85}$Se/Ni$_{0.85}$Se	250	10	93	17
NiFeP/NCH	216	10	—	18
FeCo/Co$_2$P@NPCF	260	10	120	19
SWCNTs/ReS$_2$	327	10	—	20
Co^{II}Fe-ONC	284	10	75.8	21
Pd-e-NiCo-PBA-C	147	10	67	22
Fe-Co-Ni-P-1	215	10	72.1	23

Table S4 Fitting parameters of Fe_2P/Ni_2P electrode for impedance spectra in **Fig. 6a**.

Potential (V)	R_1 (Ω)	R_2 (Ω)
1.20	4845	1336
1.25	4676	1267
1.30	4426	1205
1.35	4230	937
1.40	2612	239.3
1.45	1235	15.6
1.50	162.8	7.4
1.55	28	6.2
1.60	15	5.1

Table S5 Fitting parameters of Fe_2P/Ni_5P_4 electrode for impedance spectra in **Fig. 6d.**

Potential (V)	R_1 (Ω)	R_2 (Ω)
1.20	11569	2774
1.25	10385	2673
1.30	10194	2543
1.35	9945	2204
1.40	6769	975
1.45	2684	674
1.50	300	101
1.55	63	31
1.60	19	5.6

Table S6 Comparison of OER performance in alkaline seawater solution for Fe_2P/Ni_2P with some representative catalysts reported.

Catalysts	Overpotential (mV)	Current density (mA cm^{-2})	Tafel slope (mV/dec)	Ref.
Fe_2P/Ni_2P	**229**	**10**	**89.3**	**This work**
Fe_2P-NiCoP	258	10	49	24
FCNP@CQs	268	10	45.2	25
$CoSe_2$-NCF	245	10	93	26
Er-MoO_2	312	10	99	27
ER-SNCF-20s	278	10	57	28
Fe_2P-NiCoP	245	10	82.5	29
NiMoSe@CC	360	10	—	30
$Co_2P/CoMoP_2$	268	10	81	31

Table S7 The alkaline OWS performance of Fe_2P/Ni_2P with some representative bifunctional electrocatalysts reported.

Catalysts	Electrolyte	Cell voltage (V)	Ref
Fe_2P/Ni_2P	1.0 KOH	**1.63**	**This work**
S,N-CNTs /CoS_2@Co	1.0 KOH	1.633	32
CoNSC	1.0 KOH	1.64	33
CoP/NCNHP	1.0 KOH	1.64	34
Co/β-Mo_2C@N-CNTs	1.0 KOH	1.64	35
CoP@SNC	1.0 KOH	1.64	36
v- NiS_2/CeO_2	1.0 KOH	1.64	37
Ni/Mo_2C-NCNF	1.0 KOH	1.64	38
Co_9S_8/WS_2/Ti foil	1.0 KOH	1.65	39
CoP	1.0 KOH	1.65	40
$NiCo_2O_4$	1.0 KOH	1.65	41
ONPPGC/OCC	1.0 KOH	1.66	42
EG/$Co_{0.85}$Se/NiFe LDH	1.0 KOH	1.67	43
Co-NC/C	1.0 KOH	1.67	44
Sv-Co_3S_4/MoS_2	1.0 KOH	1.67	45
FeCo/Co_2P@C	1.0 KOH	1.68	19
NiFe LDH/NF	1.0 KOH	1.7	46
Ni_5Ni_4/NF	1.0 KOH	1.7	47
Co_9S_8/Ni_3S_2/NF	1.0 KOH	1.743	48
Ni_3S_2	1.0 KOH	1.76	49
$Ni(OH)_2$/CC//$NiSe_2$/CC	1.0 KOH	1.78	50

References

1. Y. Chen, Z. Yang, J. Wang, Y. Yang, X. He, Y. Wang, J. Chen, Y. Guo, X. Wang, S. Wang, *Nano Res.* 2023, **1**.

2. Q. P. Ngo, T. T. Nguyen, Q. T. T. Le, J. H. Lee, N. H. Kim, *Adv. Energy Mater.* 2023, **13**, 2301841.

3. M. Bi, Y. Zhang, X. Jiang, J. Sun, X. Wang, J. Zhu, Y. Fu, *Adv. Energy Mater.* 2024, **34**, 2309330.

4. C. Lyu, C. Cao, J. Cheng, Y. Yang, K. Wu, J. Wu, W.-M. Lau, P. Qian, N. Wang, J. Zheng, *Chem. Eng. J.* 2023, **464**, 142538.

5. A. Ren, B. Yu, M. Huang, Z. Liu, *I Int. J. Hydrogen Energy.* 2024, **51**, 490.

6. X. Fu, Z. Zhang, Y. Zheng, J. Lu, S. Cheng, J. Su, H. Wei, Y. Gao, *J. Colloid Interf. Sc*i. 2024, **653**, 1272.

7. S. Liu, Z. Lin, R. Wan, Y. Liu, Z. Liu, S. Zhang, X. Zhang, Z. Tang, X. Lu, Y. Tian, *J. Mater. Chem.* A. 2021, **9**, 21259.

8. L. Wang, Q. Zhou, Z. Pu, Q. Zhang, X. Mu, H. Jing, S. Liu, C. Chen, S. Mu, *Nano Energy.* 2018, **53**, 270.

9. K. Liu, C. Zhang, Y. Sun, G. Zhang, X. Shen, F. Zou, H. Zhang, Z. Wu, E. C. Wegener, C. J. Taubert, *ACS Nano,* **2018**, **12**, 158.

10. Y. Liu, N. Ran, R. Ge, J. Liu, W. Li, Y. Chen, L. Feng, R. Che, *Chem. Eng. J.* 2021, **425**, 131642.

11. R. Zhang, Z. Wei, G. Ye, G. Chen, J. Miao, X. Zhou, X. Zhu, X. Cao, X. Sun, *Adv. Energy Mater*. 2021, **11**, 2101758.

12. J.-B. Chen, J. Ying, Y.-X. Xiao, G. Tian, Y. Dong, L. Shen, S. I. Córdoba de Torresi, M. D. Symes, C. Janiak, X.-Y. Yang, *ACS Catal*. 2023, **13**, 14802.

13. J. Bao, Y. Zhou, Y. Zhang, X. Sheng, Y. Wang, S. Liang, C. Guo, W. Yang, T. Zhuang, Y. Hu, *J. Mater. Chem. A*. 2020, **8**, 22181.

14. S. Bolar, S. Shit, J. S. Kumar, N. C. Murmu, R. S. Ganesh, H. Inokawa, T. Kuila, *Appl. Catal. B: Environ. Energ*y, 2019, **254**, 432.

15. T. Liang, S. Lenus, Y. Liu, Y. Chen, T. Sakthivel, F. Chen, F. Ma, Z. Dai, *Energy Environ. Mater.* **2023**, **6**, e12332.

16. W.-L. Ding, Y.-H. Cao, H. Liu, A.-X. Wang, C.-J. Zhang, X.-R. Zheng, *Rare Metal*s. 2021, **40**, 1373.

17. K. Ao, J. Dong, C. Fan, D. Wang, Y. Cai, D. Li, F. Huang, Q. Wei, *ACS sustainable Chem. Eng*. 2018, **6**, 10952.

18. Y.-S. Wei, M. Zhang, M. Kitta, Z. Liu, S. Horike, Q. Xu, *J. Am. Chem. Soc*. 2019, **141**, 7906.

19. Q. Shi, Q. Liu, Y. Ma, Z. Fang, Z. Liang, G. Shao, B. Tang, W. Yang, L. Qin, X. Fang, *Adv. Energy Mater*. 2020, **10**, 1903854.

20. B. Martín-García, D. Spirito, S. Bellani, M. Prato, V. Romano, A. Polovitsyn, R. Brescia, R. Oropesa-Nuñez, L. Najafi, A. Ansaldo, *Small*. 2019, **15**, 1904670.

21. P. Guo, Z. Wang, T. Zhang, C. Chen, Y. Chen, H. Liu, M. Hua, S. Wei, X. Lu, *Appl. Catal. B: Environ. Energ*y, 2019, **258**, 117968.

22. H. Zhang, Q. Jiang, J. H. Hadden, F. Xie, D. J. Riley, *Adv. Energy Mater.* 2021, **31**, 2008989.

23. X. Zhou, Y. Zi, L. Xu, T. Li, J. Yang, J. Tang, *Inorg. Chem.* 2021, **60**, 11661.

24. M. Xiao, C. Zhang, P. Wang, W. Zeng, J. Zhu, Y. Li, W. Peng, Q. Liu, H. Xu, Y. Zhao, *Mater. Today Phys*. 2022, **24**, 100684.

25. S. Lv, Y. Deng, Q. Liu, Z. Fu, X. Liu, M. Wang, Z. Xiao, B. Li, L. Wang, *Appl. Catal. B: Environ. Energ*y. 2023, **326**, 122403.

26. H. Chen, S. Zhang, Q. Liu, P. Yu, J. Luo, G. Hu, X. Liu, *Inorg. Chem. Commun.* 2022, **146**, 110170.

27. T. Yang, H. Lv, Q. Quan, X. Li, H. Lu, X. Cui, G. Liu, L. Jiang, *Appl. Surf. Sci.* 2023, **615**, 156360.

28. R. Hu, M. Zhao, H. Miao, F. Liu, J. Zou, C. Zhang, Q. Wang, Z. Tian, Q. Zhang, J. Yuan, *Nanoscale.* 2022, **14**, 10118.

29. L. Jin, H. Xu, K. Wang, L. Yang, Y. Liu, X. Qian, G. He, H. Chen, *Appl. Surf. Sci.* 2024, 159777.

30. M. Saquib, P. Arora, A. C. Bhosale, *Fuel.* 2024, **365**, 131251.

31. B. Sun, C. Li, J. Yang, H. Bai, X. Meng, *Inorg. Chem. Front.* 2024.

32. J.-Y. Wang, T. Ouyang, N. Li, T. Ma, Z.-Q. Liu, *Sci. Bull.* 2018, **63**, 1130.

33. Z. Zhang, X. Zhao, S. Xi, L. Zhang, Z. Chen, Z. Zeng, M. Huang, H. Yang, B. Liu, S. J. Pennycook, *Adv. Energy Mater.* 2020, **10**, 2002896.

34. Y. Pan, K. Sun, S. Liu, X. Cao, K. Wu, W.-C. Cheong, Z. Chen, Y. Wang, Y. Li, Y. Liu, *J. Am. Chem. Soc.* 2018, **140**, 2610.

35. T. Ouyang, Y. Q. Ye, C. Y. Wu, K. Xiao, Z. Q. Liu, A*ngew. Chem. Int. Ed.* 2019, **58**, 4923.

36. T. Meng, Y.-N. Hao, L. Zheng, M. Cao, *Nanoscale* 2018, **10**, 14613.

37. W. Liao, W. Li, Y. Zhang, *Mater. Today Chem.* 2022, **24**, 100791.

38. M. Li, Y. Zhu, H. Wang, C. Wang, N. Pinna, X. Lu, *Adv. Energy Mater.* 2019, **9**, 1803185.

39. S. Peng, L. Li, J. Zhang, T. L. Tan, T. Zhang, D. Ji, X. Han, F. Cheng, S. Ramakrishna, *J. Mater. Chem. A.* 2017, **5**, 23361.

40. L. Ji, J. Wang, X. Teng, T. J. Meyer, Z. Chen, *ACS Catal.* 2019, **10**, 412.

41. X. Gao, H. Zhang, Q. Li, X. Yu, Z. Hong, X. Zhang, C. Liang, Z. Lin, *Angew. Chem. Int. Ed.* 2016, **55**, 6290.

42. J. Lai, S. Li, F. Wu, M. Saqib, R. Luque, G. Xu, *Energy Environ. Sci.* 2016, **9**, 1210.

43. Y. Hou, M. R. Lohe, J. Zhang, S. Liu, X. Zhuang, X. Feng, *Energy Environ. Sci.* **2**016, **9**, 478.

44. H. Huang, S. Zhou, C. Yu, H. Huang, J. Zhao, L. Dai, J. Qiu, *Energy Environ. Sci.* 2020, 13, 545.

45. Q. He, N. Ye, L. Han, K. Tao, *Inorg. Chem.* 2023, **62**, 21240.

46. J. Luo, J.-H. Im, M. T. Mayer, M. Schreier, M. K. Nazeeruddin, N.-G. Park, S. D. Tilley, H. J. Fan, M. Grätzel, *Sci.* 2014, **345**, 1593.

47. M. Ledendecker, S. Krick Calderón, C. Papp, H. P. Steinrück, M. Antonietti, M. Shalom, *Angew. Chem. Int. Ed.* 2015, 54, 12361.

48. Y. Yang, H. Yao, Z. Yu, S. M. Islam, H. He, M. Yuan, Y. Yue, K. Xu, W. Hao, G. Sun, *J. Am. Chem. Soc.* 2019, **141**, 10417.

49. L.-L. Feng, G. Yu, Y. Wu, G.-D. Li, H. Li, Y. Sun, T. Asefa, W. Chen, X. Zou, *J. Am. Chem. Soc.* 2015, **137**, 14023.

50. H. Liang, L. Li, F. Meng, L. Dang, J. Zhuo, A. Forticaux, Z. Wang, S. Jin, *Chem. Mater.* 2015, **27**, 5702.